Article:
Hooper, TE and Bell, AJ orcid.org/0000-0002-2061-3862 (2020) Landau–Devonshire derived phase diagram of the BiFeO3–PbTiO3 solid solution. Journal of Applied Physics, 127 (10). 104102. ISSN 0021-8979

https://doi.org/10.1063/1.5144151

Landau-Devonshire Derived Phase Diagram of the $BiFeO_3$-$PbTiO_3$ Solid Solution

T. E. Hooper & A. J. Bell

Abstract

Since the construction of the first structural phase diagram of the $BiFeO_3$-$PbTiO_3$ solid solution, there has been ambiguity as to the true location of the morphotropic phase boundary. In this study a Landau-Devonshire (LD) derived phase diagram has been constructed in order to provide a mathematically derived perspective. The compositional dependence on properties has been modelled as a linear dependence between the landau coefficients of each end member. It is found that the only structural phases found below T_C are rhombohedral and tetragonal which at 25˚C shows an MPB at $0.696BiFeO_3$-$0.304PbTiO_3$. The MPB also shows a temperature dependence similar to other ferroelectric solid solutions in which the tetragonal-rhombohedral phase transition moves towards higher $BiFeO_3$ contents at higher temperatures. Although the replication of the experimentally observed phase diagram can be constructed, this method is found to be insufficient for describing the spontaneous strain behaviour.

[Key words: Thermodynamics, bismuth ferrite lead titanate, phase diagram, Landau-Devonshire]

1 Introduction

The solid solution between rhombohedral $BiFeO_3$ and tetragonal $PbTiO_3$ is of great scientific and technological interest due it's large T_C compared to market dominant $Pb(Zr,Ti)O_3$ [1], the ability to exhibit multiferroic behaviour at room temperature [2, 3, 4, 5] and analogous to high-performance piezoelectric materials possesses a morphotropic phase boundary (MPB) [1, 6]. However the compositional location of this structural phase transition from a rhombohedral-tetragonal coexistence to pure rhombohedral phase is ambiguous with different values being reported. The initial phase diagram constructed by Fedulov et al. [1] shows a rhombohedral-tetragonal mixed phase region spanning from 66mol% to 73mol% $BiFeO_3$. Since then, Woodward et al. [7] have reported a mixed phase region from 60-70mol% $BiFeO_3$, Sunder et al. [8] found the MPB to be located between 70-80mol% $BiFeO_3$ and Bell et al. [9] found a rhombohedral-tetragonal coexistence from 40-70mol% $BiFeO_3$. Other reported locations for the MPB are between 67-71mol% [10], 60-80mol% [4] and 72-82mol% $BiFeO_3$ [11]. The discrepancy between values originates from the extremely large spontaneous strain which results in large internal stresses and high sensitivity to sample form, processing and preparation conditions which can influence and distort x-ray diffraction patterns and therefore the location of the MPB [7, 9]. Factors such as intergranular stresses imparted on by grinding and polishing, crushing and annealing can all have a significant impact on structural characterisation.

Here, LD theory has been applied in order to shed light on the location of the MPB from a theoretical, thermodynamic perspective and thus avoids the complexities associated with influences stemming from material processing.

2 Methodology

Landau-Devonshire (LD) theory has been a useful and powerful tool since it was first applied to ferroelectrics in the mid-20th century [12, 13] and remains relevant today. LD theory considers the free energy of a ferroelectric within the vicinity of a phase transition as a function of temperature, field, stress and an order parameter. The order parameter represents a value which is zero in the high-symmetry phase and non-zero in the lower symmetry phase [14] and is usually taken as the macroscopic polarisation.

The LD free energy (ΔG) of a single domain, single crystal truncated to the sixth-order can be expressed as shown in Equation (1).

$$\begin{aligned}\Delta G_{total} = {} & \alpha_1(P_1^2 + P_2^2 + P_3^2) + \alpha_{11}(P_1^4 + P_2^4 + P_3^4) + \alpha_{12}(P_1^2P_2^2 + P_2^2P_3^2 + P_3^2P_1^2) + \alpha_{111}(P_1^6 + P_2^6 + P_3^6) \\ & + \alpha_{112}(P_1^4[P_2^2 + P_3^2] + P_2^4[P_1^2 + P_3^2] + P_3^4[P_1^2 + P_2^2]) + \alpha_{123}(P_1^6P_2^6P_3^6) \\ & - \frac{1}{2}s_{11}^P(X_1^2 + X_2^2 + X_3^2) - s_{12}^P(X_1X_2 + X_2X_3 + X_3X_1) - \frac{1}{2}s_{44}^P\left(X_4^2 + X_5^2 + X_6^2\right) \\ & - Q_{11}(X_1P_1^2 + X_2P_2^2 + X_3P_3^2) + Q_{12}[X_1(P_2^2 + P_3^2) + X_2(P_1^2 + P_3^2) + X_3(P_1^2 + P_2^2)] \\ & - Q_{44}(X_4P_2P_3 + X_5P_1P_3 + X_6P_1P_2) - E_1P_1 - E_2P_2 - E_3P_3\end{aligned} \tag{1}$$

Where P_i are the orthogonal polarisation components, α_{ijk} are the dielectric stiffness or Landau coefficients, s_{ij} are the elastic compliances, X_i is stress, Q_{ij} are the electrostriction coefficients and E_i is electric field.

For a stress-free (X_i=0) single crystal in the absence of an electric field (E_i=0), the solutions to Equation (1) are structurally dependent and are shown in Equation (2) for the cubic, tetragonal, orthorhombic and rhombohedral phases.

$$\begin{aligned}&\text{Cubic - } P_1 = P_2 = P_3 = 0 \\ &\text{Tetragonal - } P_1 = P_2 = 0; P_3 \neq 0 \\ &\text{Orthorhombic - } P_1 = 0; P_2 = P_3 \neq 0 \\ &\text{Rhombohedral - } P_1 = P_2 = P_3 \neq 0\end{aligned} \tag{2}$$

It is worth noting that the monoclinic phase has not been considered in this study due to the limitations in the available Landau coefficients which require dielectric stiffness coefficients up to the eighth order to be evaluated. By applying the conditions in Equation (2) to Equation (1), the free energy functions for each structural phase can be determined:

$$\Delta G_{cubic} = 0$$

$$\Delta G_{tet} = \alpha_1 P_3^2 + \alpha_{11} P_3^4 + \alpha_{111} P_3^6$$

$$\Delta G_{orth} = \alpha_1 (P_2^2 + P_3^2) + \alpha_{11} (P_2^4 + P_3^4) + \alpha_{12} (P_2^2 P_3^2) + \alpha_{111} (P_2^6 + P_3^6) + \alpha_{112} (P_2^4 P_3^2 + P_3^4 P_2^2)$$

$$\Delta G_{rhom} = \alpha_1 (P_1^2 + P_2^2 + P_3^2) + \alpha_{11} (P_1^4 + P_2^4 + P_3^4) + \alpha_{12} (P_1^2 P_2^2 + P_2^2 P_3^2 + P_1^2 P_3^2) + \alpha_{111} (P_1^6 + P_2^6 + P_3^6) + \alpha_{112} (P_1^4 [P_2^2 + P_3^2] + P_2^4 [P_1^2 + P_3^2] + P_3^4 [P_1^2 + P_2^2]) + \alpha_{123} P_1^2 P_2^2 P_3^2 \quad (3)$$

By using the appropriate structurally dependent conditions listed in Equation (2) and minimising the free energy ($\partial G/\partial P_i = 0$), the values for the spontaneous polarisation components can be determined using the quadratic relation:

$$P^2 = \frac{-b \pm \sqrt{b^2 - 4ac}}{2a} \quad (4)$$

$$\text{Tetragonal - } a = \alpha_1; b = 2\alpha_{11}; c = 3\alpha_{111}$$

$$\text{Orthorhombic - } a = \alpha_1;\ b = 2\alpha_{11} + \alpha_{12};\ c = 3\alpha_{111} + 3_{112}$$

$$\text{Rhombohedral - } a = \alpha_1;\ b = 2\alpha_{11} + 2\alpha_{12};\ c = 3\alpha_{111} + 6\alpha_{112} + \alpha_{123} \quad (5)$$

The elastic spontaneous strain is calculated by differentiating the free energy as a function of stress ($\partial \Delta G/\partial X_i$):

$$\text{Cubic - } x_1 = x_2 = x_3 = x_4 = x_5 = x_6 = 0$$

$$\text{Tetragonal - } x_1 = x_2 = Q_{12} P_3^2; x_3 = Q_{11} P_3^2; x_4 = x_5 = x_6 = 0$$

$$\text{Orthorhombic - } x_1 = 2Q_{12} P_3^2; x_2 = x_3 = (Q_{11} + Q_{12}) P_3^2; x_4 = Q_{44} P_3^2; x_5 = x_6 = 0$$

$$\text{Rhombohedral - } x_1 = x_2 = x_3 = (Q_{11} + Q_{12}) P_3^2; x_4 = x_5 = x_6 = Q_{44} P_3^2 \quad (6)$$

In order to replicate the compositional-dependence of properties for the $BiFeO_3$-$PbTiO_3$ solid solution, a linear relationship was employed to extrapolate between the fourth-order and sixth-order dielectric stiffness coefficients and the electrostriction coefficients for lead titanate and bismuth ferrite taken from [15] and [16], respectively. The second-order dielectric stiffness term for lead titanate was calculated using the Curie-Weiss constant taken from [15] and for bismuth ferrite was determined using linear extrapolation of the Curie-Weiss constant against Curie temperature for unary perovskites [17] using the accepted value of 827°C [16]. The linear relationship between the Curie temperature of each end member is also employed. Whilst this methodology is straightforward, Heitmann and Rossetti [18] were able to replicate the experimentally observed phase diagrams for PZT, PMN-PT and PZN-PT by applying Vegard's law to T_C, the

temperature independent second-order power term (α_0) and fourth-order power term (α_{12}) between end members.

$$T_C^{BFPT} = (1-x)T_C^{PT} + (x)T_C^{BF}$$

$$C_{CW}^{BFPT} = (1-x)C_{CW}^{PT} + (x)C_{CW}^{BF}$$

$$\alpha_{11}^{BFPT} = (1-x)\alpha_{11}^{PT} + (x)\alpha_{11}^{BF}$$

$$\alpha_{12}^{BFPT} = (1-x)\alpha_{12}^{PT} + (x)\alpha_{12}^{BF}$$

$$\alpha_{111}^{BFPT} = (1-x)\alpha_{111}^{PT} + (x)\alpha_{111}^{BF}$$

$$\alpha_{112}^{BFPT} = (1-x)\alpha_{112}^{PT} + (x)\alpha_{112}^{BF}$$

$$\alpha_{123}^{BFPT} = (1-x)\alpha_{123}^{PT} + (x)\alpha_{123}^{BF}$$

$$Q_{11}^{BFPT} = (1-x)Q_{11}^{PT} + (x)Q_{11}^{BF}$$

$$Q_{12}^{BFPT} = (1-x)Q_{12}^{PT} + (x)Q_{12}^{BF}$$

$$Q_{44}^{BFPT} = (1-x)Q_{44}^{PT} + (x)Q_{44}^{BF} \quad (7)$$

Table 1: Landau coefficients used for $PbTiO_3$ and $BiFeO_3$

Coefficient	$PbTiO_3$	$BiFeO_3$
T_C ($^\circ C$)	492.2	827
C_{CW} (10^5 $^\circ C$–1)	1.50	2.04*
α_{11} ($10^7 m^5/[C^2.F]$)	-7.252	22.9
α_{12} ($10^8 m^5/[C^2.F]$)	7.5	3.06
α_{111} ($10^8 m^9/[C^4.F]$)	2.606	0.599
α_{112} ($10^8 m^9/[C^4.F]$)	6.1	-0.000334
α_{123} ($10^9 m^9/[C^4.F]$)	-3.66	-0.178
Q_{11} ($10^{-2} m^4/C^2$)	0.089	0.032
Q_{12} ($10^{-2} m^4/C^2$)	-0.026	-0.016
Q_{44} ($10^{-2} m^4/C^2$)	0.0675	0.02
Ref.	[15]	[16], *[17]

3 Results & Discussion

Figure 1 shows the free energy as a function of temperature for (x)$BiFeO_3$-(1-x)$PbTiO_3$ where x=0.60, 0.65, 0.675, 0.70, 0.75 and 0.80 for the rhombohedral, orthorhombic and tetragonal phases. As well as the location of the MPB, there is also debate as to which structural phases are present. Previous reports [4] have observed a tetragonal-rhombohedral-orthorhombic coexistence at the MPB using conventional x-ray diffraction. Further evidence for the presence of a possible orthorhombic phase was postulated from

electron diffraction studies which showed additional reflections to those of the rhombohedral and tetragonal phases suggesting the presence of a lower symmetry phase [7]. However Reitveld refinement of x-ray powder diffractions by Bhattacharjee et al. [10] show that the MPB consists of a tetragonal-monoclinic coexistence, showing no evidence for the presence of a rhombohedral or orthorhombic phase. In this study, the line which represents the free energy of the orthorhombic phase always lies above those of the rhombohedral and tetragonal phases, indicating that it is an unstable or metastable phase for the compositions shown in Figure 1.

For compositions where x=0.60, 0.65 and 0.675, the most stable structural phase is always tetragonal with no intermediate ferroelectric-ferroelectric phase transitions occurring between 0˚C and T_C. For x=0.70 a rhombohedral-tetragonal phase transition occurs at approximately 40˚C and remains tetragonal until T_C. At compositions x=0.75 and x=0.80, this transition occurs at higher temperatures suggesting a temperature dependent MPB.

Using the results from Figure 1, a phase diagram is constructed by calculating the difference in free energies of the rhombohedral and tetragonal phases over all compositions and temperatures.

$$\Delta G = |G_{tet}| - |G_{rhom}| \tag{8}$$

On this basis, it is assumed that a stable tetragonal phase is present when ΔG >0, a rhombohedral phase is present at ΔG <0 and a morphotropic phase boundary is present at ΔG =0 where there is a degeneracy in energy states between the two.

Figure 2 shows the thermodynamically derived phase diagram of $BiFeO_3$-$PbTiO_3$ calculated using Equation (8). According to Figure 2 the location of the MPB at 25˚C is x=0.696 showing good agreement with previously quoted values of x=0.70 [7, 9, 10]. Furthermore as LD theory assumes a macroscopic polarisation of a single-domain single crystal, it is unsurprising that Figure 2 demonstrates a sharp MPB with no broad mixed phase region. Although this is contrary to many studies on polycrystalline $BiFeO_3PbTiO_3$, the phenomenon of phase coexistence has been shown to be grain size related [19] with samples possessing larger grains and single crystals exhibiting pure tetragonal and rhombohedral structures at either side of the MPB [20, 21, 22].

Figure 3 shows the spontaneous strain as a function of composition at 25˚C. According to this work the spontaneous strain decreases from pure lead titanate towards the MPB, at which point the axial (x_3) and lateral (x_1) strain 'collapse' when a rhombohedral phase is formed and the lattice parameters become equal. Within the rhombohedral region, the axial and lateral strain increase from 0.0% for pure $BiFeO_3$ to 0.20% at the MPB and shear strain ($x_{4,5,6}$) increase from 0.42% for $BiFeO_3$ to 0.61% at the MPB. Whilst the location of the MPB and the structural phases that are present within it are ambiguous, the almost exclusive spontaneous strain behaviour in $BiFeO_3$-$PbTiO_3$ within the tetragonal region is widely accepted [4, 7, 8, 9, 10]. Typical MPB containing ferroelectric solid solutions show spontaneous strain behaviour analogous to that shown in Figure 3, however in $BiFeO_3$-$PbTiO_3$ it is observed to increase with decreasing lead titanate content reaching approximately 18% at 70mol% $BiFeO_3$.

It is also worth mentioning that the validity of the Landau coefficients which are often extrapolated from a single experimental dataset and therefore can be limited for general use. For example coefficients that are interpolated from experimental data from a $BiFeO_3$ thin film may be suitable for the individual experiment and potentially to other $BiFeO_3$ thin films. However they may not be suitable for describing other systems such as polycrystalline and/or single crystal systems. Whilst the Landau coefficients for $PbTiO_3$ are an established set, to the author's knowledge the Landau coefficients from [16] have not been used since the original work. The agreement between experimental and theoretical phase diagrams highlights the validity of the $BiFeO_3$ coefficients for general use and may be useful in providing a theoretical description of other ferroelectric solid solutions containing a $BiFeO_3$ end member.

The ability to construct a structural phase diagram that is somewhat in agreement with experimental observations whilst incorrectly describing the spontaneous strain behaviour may shed light on the validity of applying Vegard's law to the Landau coefficients of each end member. The free energy of rhombohedral and tetragonal phases may be primarily dictated by the second and sixth-order terms in Equation (1), and Figure 2 suggests that applying a linear relation to model the compositional-dependence of these coefficients between each end member is valid. The inability to accurately describe the spontaneous strain behaviour in Figure 3 implies that applying a linear relationship between the fourth-order power terms, which dictates the spontaneous strain, may be over-simplified and invalid. A deeper understanding of the dynamics of fourth-order coefficients may be achieved through experimental means as in Refs. [24, 25] or through the exploration of more complex relationships as in Ref. [18].

4 Conclusions

An LD derived structural phase transition for the $BiFeO_3$-$PbTiO_3$ solid solution has been constructed. The compositional dependence of the solid solution was treated as a linear relation between the Curie-Weiss constant, fourth-order and sixth-order dielectric stiffness coefficients and electrostriction coefficients of the end members. Initial results show no orthorhombic phase is present at compositions containing 60, 65, 67.5, 70, 75 and 80mol% $BiFeO_3$ at any temperature. By simultaneously solving and evaluating the free energy for the rhombohedral and tetragonal phases, a complete phase diagram was constructed showing the MPB was found to be located at $0.696BiFeO_3$-$0.304PbTiO_3$ at 25˚C and showed a temperature dependence. However the methodology used in this study is unable to describe the spontaneous strain behaviour of $BiFeO_3$-$PbTiO_3$. This introduces limitations with regard to the validity of further calculated properties. If we cannot describe properties that we already know, how valid is it to describe properties that we do not know? Efforts are currently being made to overcome this issue and calculate piezoelectric and dielectric properties.

Acknowledgements

The authors gratefully acknowledge the Engineering and Physical Sciences Research Council (EPSRC) and Thales UK Ltd for their financial support.

References

[1] S. A. Fedulov, P. B. Ladyzhinskii, I. L. Pyatigorskaya, and Y. N. Venevtsev. Complete phase diagram of the $PbTiO_3$-$BiFeO_3$ system. *Soviet Physics-Solid State*, 6(2):375–378, 1964.

[2] R. Wongmaneerung, P. Jantaratana, R. Yimnirun, and S. Ananta. Phase formation and magnetic properties of bismuth ferrite–lead titanate multiferroic composites. *Journal of Superconductivity and Novel Magnetism*, 26(2):371–379, 2013.

[3] T. Stevenson, T. P. Comyn, A. Daoud-Aladine, and A. J. Bell. Change in periodicity of the incommensurate magnetic order towards commensurate order in bismuth ferrite lead titanate. *Journal of Magnetism and Magnetic Materials*, 322(22):L64–L67, 2010.

[4] W. M. Zhu, H. Y. Guo, and Z. G. Ye. Structural and magnetic characterization of multiferroic $(BiFeO_3)_{1-x}$-$(PbTiO_3)_x$ solid solutions. *Physical Review B*, 78(1):014401, 2008.

[5] T. P. Comyn, T. Stevenson, M. Al-Jawad, G. André, A. J. Bell, and R. Cywinski. Antiferromagnetic order in tetragonal bismuth ferrite–lead titanate. *Journal of Magnetism and Magnetic Materials*, 323(21):2533–2535, 2011.

[6] D. A. Berlincourt, C. Cmolik, and H. Jaffe. Piezoelectric properties of polycrystalline lead titanate zirconate compositions. *Proceedings of the IRE*, 48(2):220–229, 1960.

[7] D. I. Woodward, I. M. Reaney, R. E. Eitel, and C. A. Randall. Crystal and domain structure of the $BiFeO_3$–$PbTiO_3$ solid solution. *Journal of Applied Physics*, 94(5):3313–3318, 2003.

[8] V. V. S. S. S. Sunder, A. Halliyal, and A. M. Umarji. Investigation of tetragonal distortion in the $PbTiO_3$–$BiFeO_3$ system by high-temperature x-ray diffraction. *Journal of Materials Research*, 10(5):1301–1306, 1995.

[9] A. J Bell, A. X. Levander, S. L. Turner, and T. P. Comyn. Internal stress and phase coexistence in bismuth ferrite-lead titanate ceramics. In *2007 Sixteenth IEEE International Symposium on the Applications of Ferroelectrics*, pages 406–409. IEEE, 2007.

[10] S. Bhattacharjee, S. Tripathi, and D. Pandey. Morphotropic phase boundary in (1- x) $BiFeO_3$– (x)$PbTiO_3$: phase coexistence region and unusually large tetragonality. *Applied Physics Letters*, 91(4):042903, 2007.

[11] V. F. Freitas, G. S. Dias, O. A. Protzek, D. Z. Montanher, I. B. Catellani, D. M. Silva, L. F. Cótica, and I. A. Dos Santos. Structural phase relations in perovskite-structured $BiFeO_3$-based multiferroic compounds. *Journal of Advanced Ceramics*, 2(2):103–111, 2013.

[12] A. F. Devonshire. XCVI. Theory of Barium Titanate: Part I. *The London, Edinburgh, and Dublin Philosophical Magazine and Journal of Science*, 40(309):1040–1063, 1949.

[13] A. F. Devonshire. CIX. Theory of Barium Titanate—Part II. *The London, Edinburgh, and Dublin Philosophical Magazine and Journal of Science*, 42(333):1065–1079, 1951.

[14] P. Chandra and P. B. Littlewood. A Landau Primer for Ferroelectrics. In *Physics of Ferroelectrics: A Modern Perspective*, pages 69–116. Heidelberg: Springer, 2007.

[15] G. A. Rossetti Jr, K. R. Udayakumar, M. J. Haun, and L. E. Cross. Thermodynamic theory of single crystal lead titanate with consideration of elastic boundary conditions. *Journal of the American Ceramic Society*, 73(11):3334–3338, 1990.

[16] Y.-H. Hsieh, F. Xue, T. Yang, H.-J. Liu, Y. Zhu, Y.-C. Chen, Q. Zhan, C.-G. Duan, L.-Q. Chen, Q. He, and Y.-H. Chu. Permanent ferroelectric retention of $BiFeO_3$ mesocrystal. *Nature Communications*, 7:13199, 2016.

[17] G. Rupprecht and R. O. Bell. Dielectric constant in paraelectric perovskites. *Physical Review*, 135(3A):A748, 1964.

[18] A. A. Heitmann and G. A. Rossetti Jr. Thermodynamics of ferroelectric solid solutions with morphotropic phase boundaries. *Journal of the American Ceramic Society*, 97(6):1661–1685, 2014.

[19] V. Kothai, B. Narayan, K. Brajesh, S. D. Kaushik, V. Siruguri, and R. Ranjan. Ferroelectric phase coexistence by crystallite size reduction in $BiFeO_3$-$PbTiO_3$. *Physical Review B*, 90(15):155115, 2014.

[20] T. L. Burnett, T. P. Comyn, and A. J. Bell. Flux growth of $BiFeO_3$–$PbTiO_3$ single crystals. *Journal of Crystal Growth*, 285(1-2):156–161, 2005.

[21] C. G. Cambridge, T. P. Comyn, T. Stevenson, and A. J. Bell. Growth and characterization of high quality $BiFeO_3$-$PbTiO_3$ single crystals. *Integrated Ferroelectrics*, 132(1):1–8, 2012.

[22] W. M. Zhu, H. Y. Guo, and Z. G. Ye. Structure and properties of multiferroic (1- x)$BiFeO_3$–(x)$PbTiO_3$ single crystals. *Journal of Materials Research*, 22(8):2136–2143, 2007.

[23] R. T. Smith, G. D. Achenbach, R. Gerson, and W. J. James. Dielectric Properties of Solid Solutions of $BiFeO_3$ with Pb(Ti, Zr)O_3 at High Temperature and High Frequency. *Journal of Applied Physics*, 39(1):70–74, 1968.

[24] M. J. Haun, E. Furman, H. A. McKinstry, and L. E. Cross. Thermodynamic theory of the lead zirconate-titanate solid solution system, part II: tricritical behavior. *Ferroelectrics*, 99(1):27–44, 1989.

[25] M. J. Haun, Z. Q. Zhuang, E. Furman, S. J. Jang, and L. E. Cross. Thermodynamic theory of the lead zirconate-titanate solid solution system, part III: Curie constant and sixth-order polarization interaction dielectric stiffness coefficients. *Ferroelectrics*, 99(1):45–54, 1989.

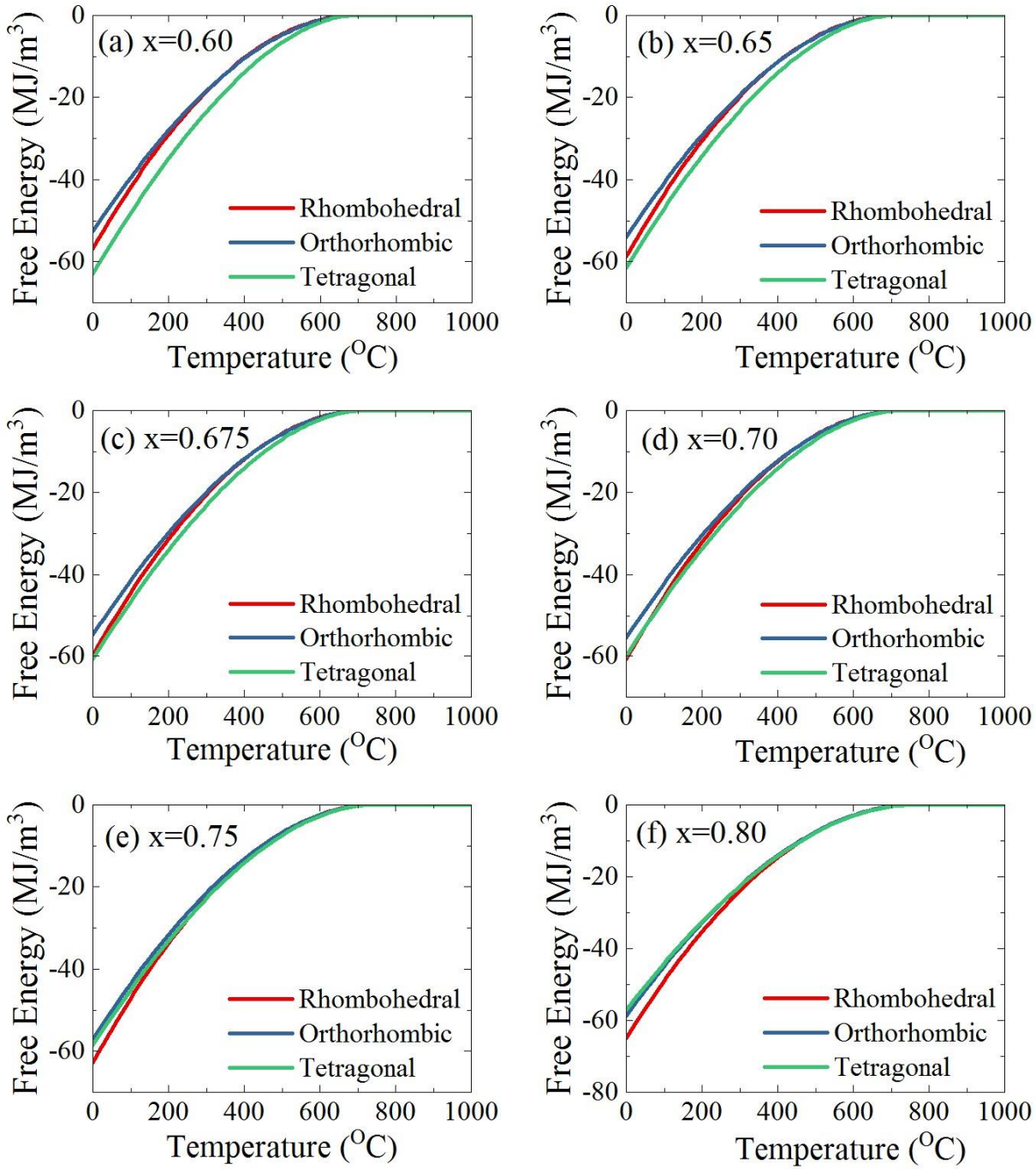

Figure 1: A comparison of the Landau-Devonshire calculated free energies in the rhombohedral, orthorhombic and tetragonal phases in (x)$BiFeO_3$-(1-x)$PbTiO_3$ for (a) x= 0.60, (b) x=0.65, (c) x=0.675, (d) x=0.70, (e) x=0.75, and (f) x=0.80

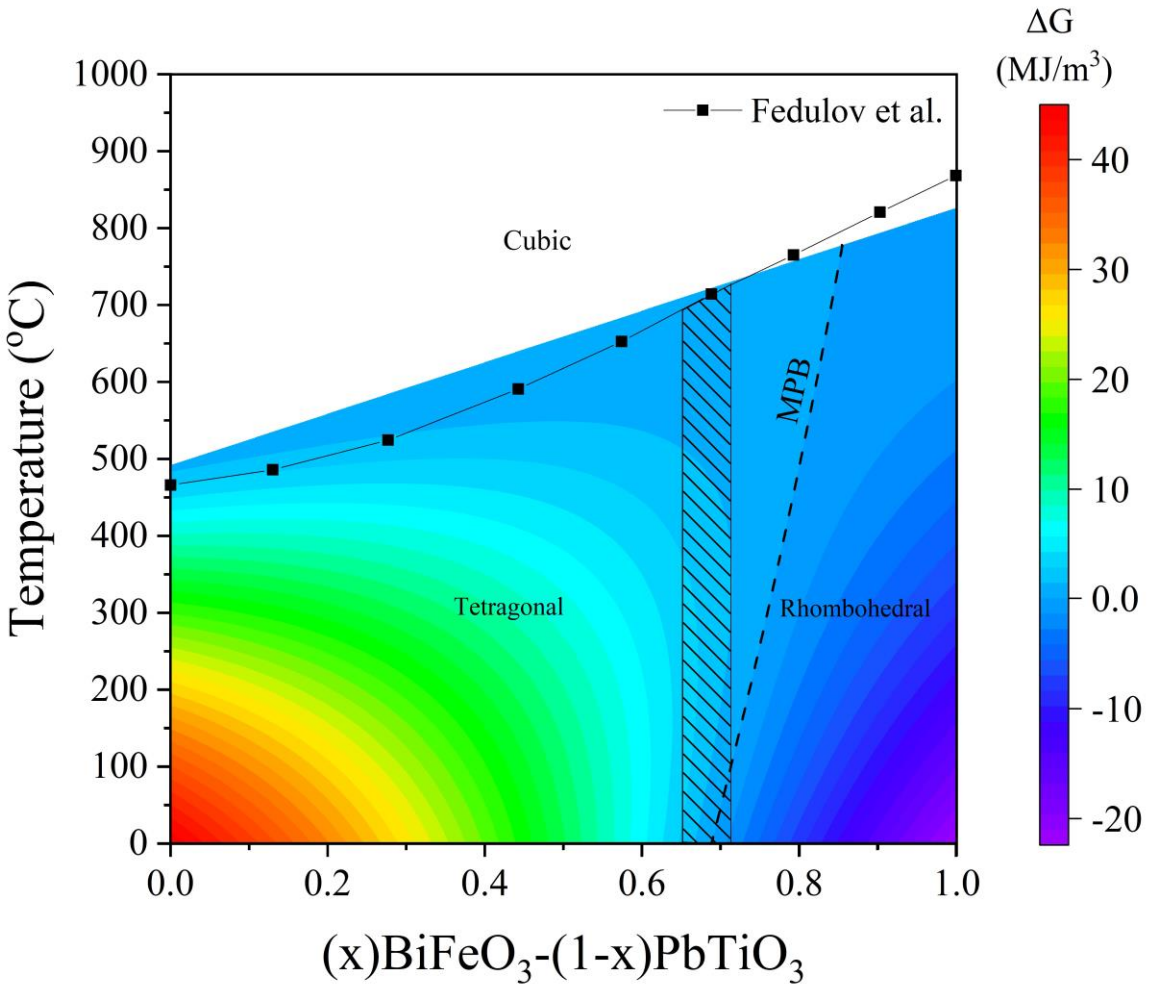

Figure 2: Landau-Devonshire derived structural phase diagram of the (x)$BiFeO_3$ - (1-x)$PbTiO_3$ Solid Solution. The original phase diagram constructed by Fedulov et al. [1] has been superimposed for comparison with the shaded area representing the region of rhombohedral-tetragonal coexistence

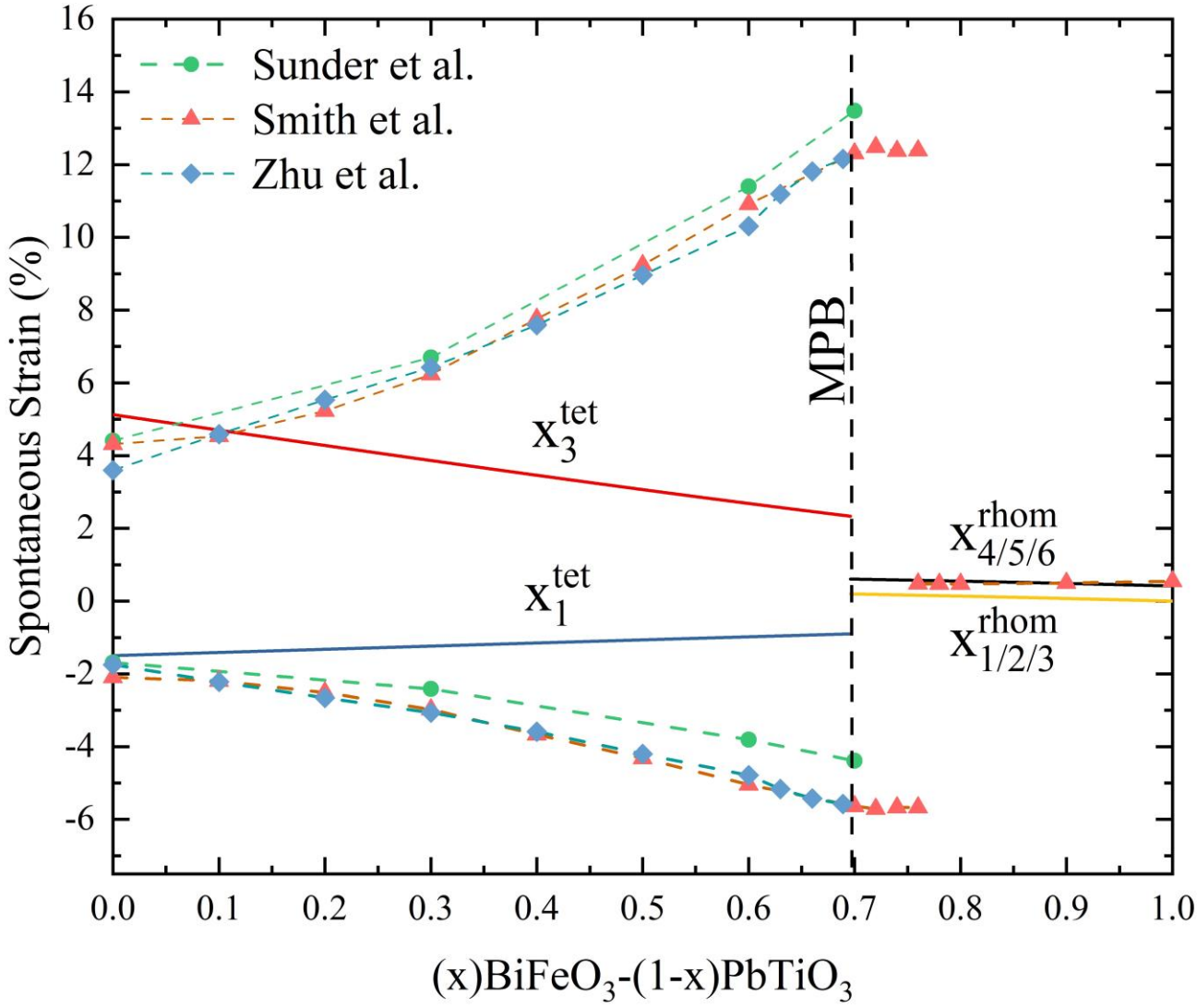

Figure 3: Landau-Devonshire derived spontaneous strain vs composition at 25°C. Experimental results from Refs. [4], [8] & [23] have been superimposed for comparison